*Electronic supplementary information (ESI)*

# Auger Process in Multilayer $WSe_2$ Crystals

*Yuanzheng Li,[a,b,#] Jia Shi,[a,e #] Heyu Chen,[b] Rui Wang,[a] Yang Mi,[a] Cen Zhang,[b] Wenna Du,[a] Shuai Zhang,[a,e] Zheng Liu,[c] Qing Zhang,[d] Xiaohui Qiu,[a] Haiyang Xu,[b,*] Weizhen Liu,[b,*] Yichun Liu,[b] and Xinfeng Liu [a,*]*

[a]Division of Nanophotonics, CAS Key Laboratory of Standardization and Measurement for Nanotechnology, CAS Center for Excellence in Nanoscience, National Center for Nanoscience and Technology, Beijing 100190, China

[b]Centre for Advanced Optoelectronic Functional Materials Research and Key Laboratory of UV-Emitting Materials and Technology (Northeast Normal University), Ministry of Education, Changchun 130024, China

[c]Center for Programmable Materials, School of Materials Science and Engineering, Nanyang Technological University, Singapore 639798, Singapore.

[d]Department of Materials Science and Engineering, College of Engineering, Peking University, Beijing 100871, China

[e]University of Chinese Academy of Sciences 19 A Yuquan Rd, Shijingshan District, Beijing, P. R. China 100049

[#]These authors contributed equally to this work.

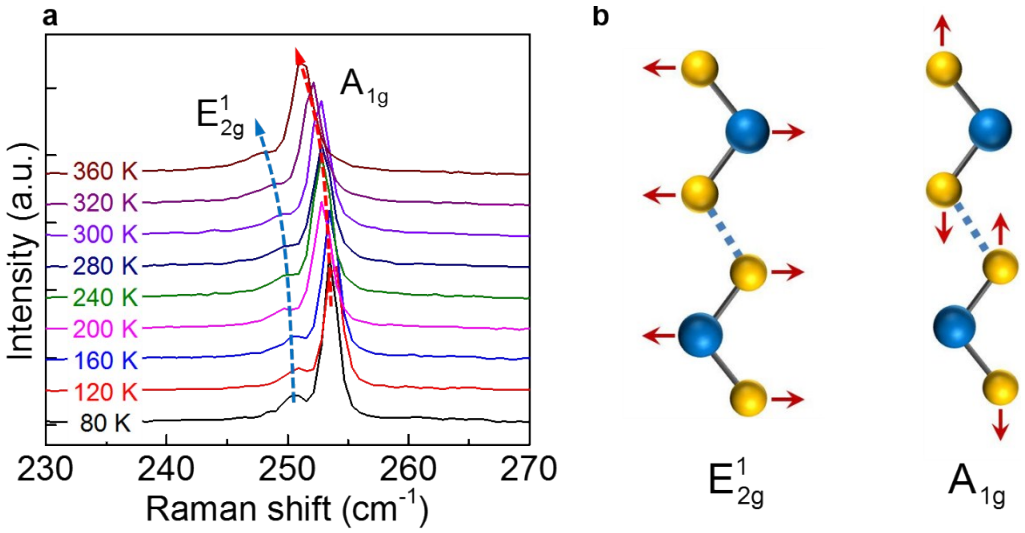


**Figure S1.** (a) Temperature dependent Raman spectra of multilayer $WSe_2$ ranging from 80 K to 360 K. The dashed blue and red lines are guides for the eye. (b) Schematic diagram of out-of-plane ($A_{1g}$) and in-plane ($E_{2g}{}^1$) Raman modes. The blue and yellow ball represents W and Se atoms, respectively.

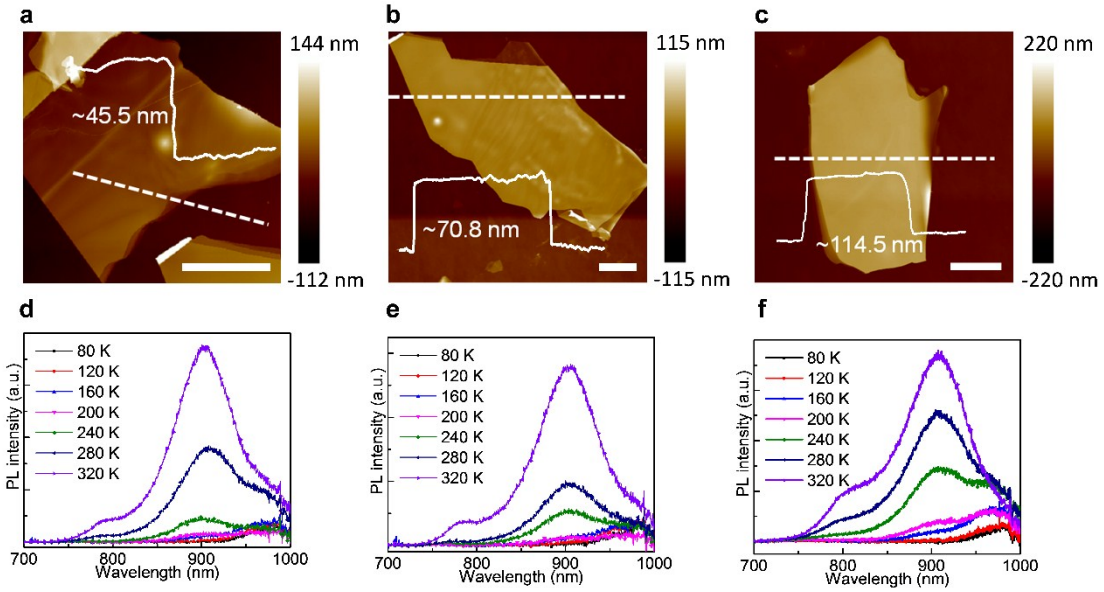


**Figure S2.** AFM images of different thickness multilayer $WSe_2$: 45.5 nm (a), 70.8 nm (b) and 114.5nm (c). Scale bar: 10 μm. Temperature dependent PL (TDPL) spectra of the three samples are shown in (d), (e) and (f), respectively. Similar PL quenching behavior are observed at low temperature in the three samples.

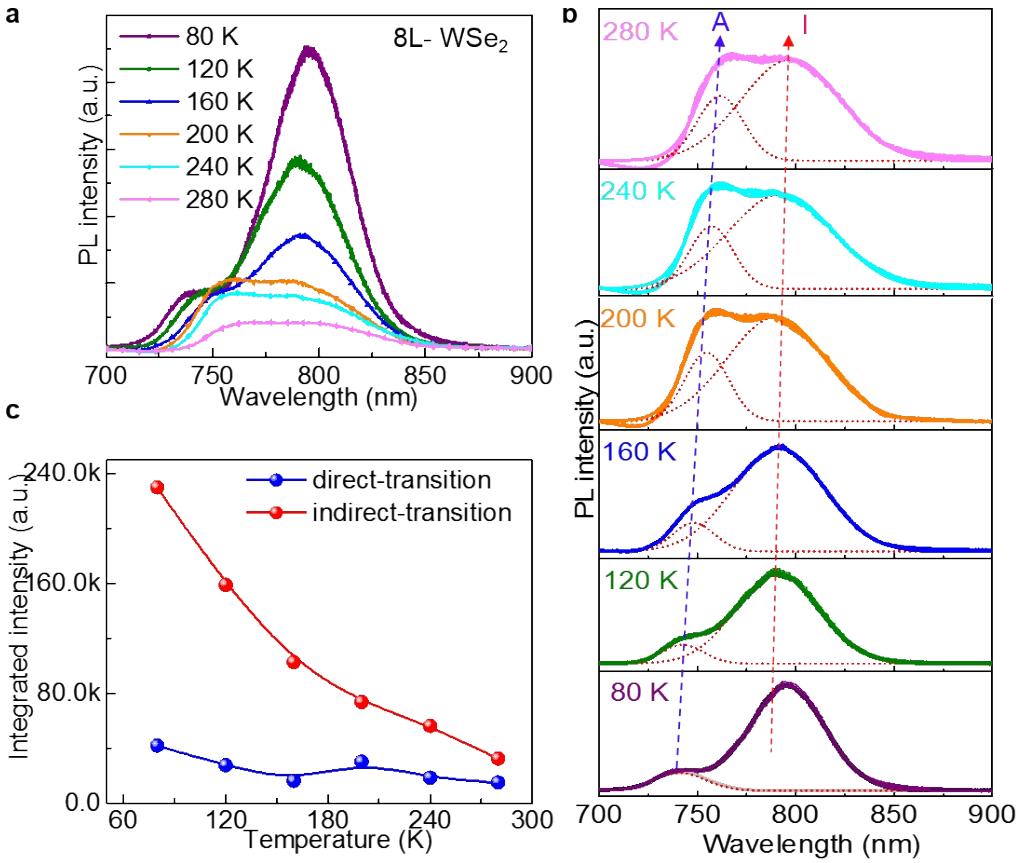


**Figure S3**. (a) Schematic diagram of bandgap structure of 8L $WSe_2$. (b) Temperature-dependent PL spectra of 8L $WSe_2$ are fitted with Gaussian peaks. The dashed blue and red lines are guides for the eye. (c) The PL integral intensity of direct transition (A) and indirect transition (I) as the function of temperature.

**Table S1.** Fitting parameters for decay curves in Figure 3b using Gaussian response function convoluted with a double exponential decay function of $Ae^{t/\tau_1} + Be^{t/\tau_2}$.

| Fluence (μJ/cm$^2$) | $\tau_1$ (fs) | A (%) | $\tau_2$ (ps) | B (%) |
|---|---|---|---|---|
| 2.44 | 619 ± 19 | 30.73 | 412.5 ± 14 | 69.27 |
| 6.58 | 532 ± 14 | 21.19 | 502.0 ± 12.6 | 78.82 |
| 9.40 | 637 ± 22 | 20.74 | 503.6 ± 13 | 79.26 |
| 15.2 | 604 ± 24 | 15.92 | 458.0 ± 10.2 | 84.08 |
| 22.6 | 732 ± 40 | 11.96 | 453.3 ± 10.8 | 88.04 |
| 30.1 | 524 ± 33 | 10.77 | 470.9 ± 10.9 | 89.23 |
| 37.6 | 426 ± 25 | 9.69 | 402.8 ± 6.6 | 90.31 |

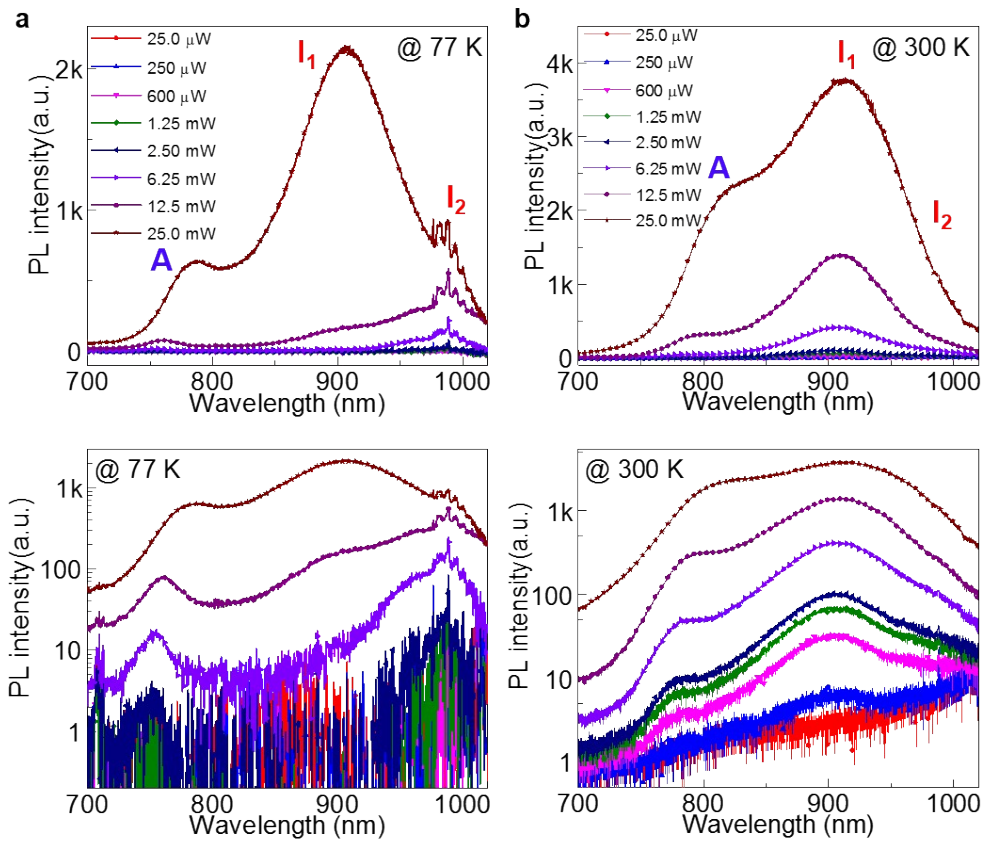


**Figure S4.** Power dependent PL (PDPL) are measured at 77 K (a) and 300 K (b). Upper panel: linear scale; Bottom panel: log scale. $I_1$ and $I_2$ indicate the indirect emission and A indicates the direct emission. The several spikes in (a) stems from laser noises and are not well deducted. These spikes of $I_2$ in (a) are noise signals which derives from 488 nm continuous-wave laser.

It should be noted that A and I1 peaks possess a significant enhancement as the pumping power increases from 12.5 mW to 25 mW. For A peak, the band structure is dependence on temperature variations based on the result of Fig. 2b. As a result, more carriers will populate in K valley and therefore the PL intensity of A peak present a significant enhancement. As for I1 peak, we consider that more phonons could reduce the carrier concentration in conduction band minimum (CBM) and valence band maximum (VBM), and meanwhile decrease the probability of Auger scattering to improve the intensity of I1 peak. Since the phonon bottleneck effect could restrict the loss of electrons and holes in our work, and induce a high carrier concentration at 77 K to increase the probability of Auger scattering. Hence, the significant enhancement

of I1 peak as the pumping power increases from 12.5 mW to 25 mW can be contributed by the broken of phonon bottleneck effect.

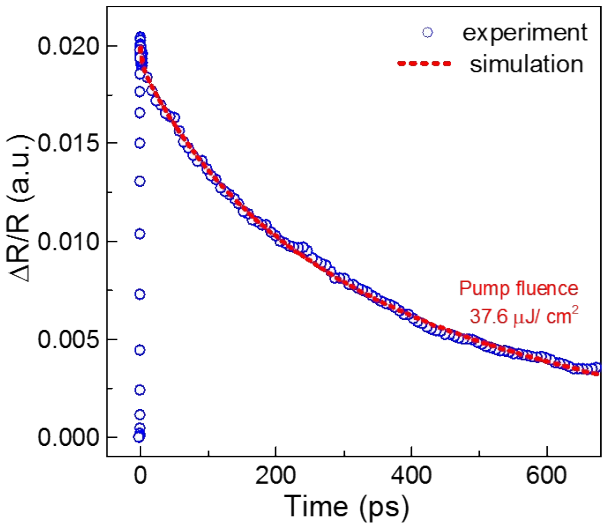


**Figure S5.** The measured (blue circle) and simulated (dashed red line) |ΔR/R| as a function of the probe delay with pump fluence of 37.6 μJ/cm$^2$. $T$ = 77 K. The two different decay processes in time scale are caused by a fast defect level and a slow defect level.

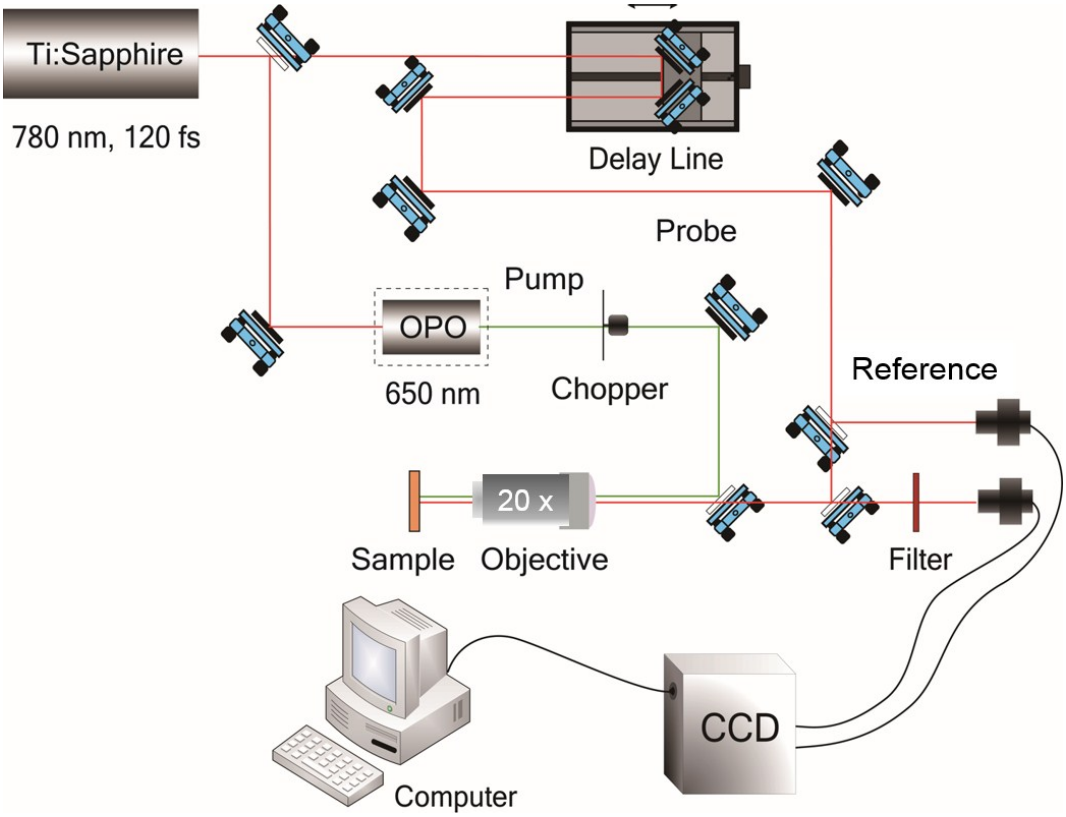


**Figure S6.** Experimental setup for the measurement of the transient absorption spectroscopy.